Nuclear Engineering and Technology 54 (2022) 681–688

Contents lists available at ScienceDirect

Nuclear Engineering and Technology

journal homepage: www.elsevier.com/locate/net

Original article

Organ dose conversion coefficients in CT scans for Korean adult males and females

Choonsik Lee [a, *], Tristan Won [b], Yeon Soo Yeom [a], Keith Griffin [a], Choonik Lee [c], Kwang Pyo Kim [d]

[a] Division of Cancer Epidemiology and Genetics, National Cancer Institute, National Institutes of Health, Rockville, MD, USA
[b] Winston Churchill High School, Potomac, MD, USA
[c] Department of Radiation Oncology, University of Michigan, Ann Arbor, MI, USA
[d] Department of Nuclear Engineering, Kyung Hee University, Gyeonggi-do, South Korea

ARTICLE INFO

Article history:
Received 23 February 2021
Received in revised form
2 August 2021
Accepted 4 August 2021
Available online 7 August 2021

Keywords:
Computed tomography
Korean voxel phantoms
Radiation dose
Monte Carlo radiation transport

ABSTRACT

Dose monitoring in CT patients requires accurate dose estimation but most of the CT dose calculation tools are based on Caucasian computational phantoms. We established a library of organ dose conversion coefficients for Korean adults by using four Korean adult male and two female voxel phantoms combined with Monte Carlo simulation techniques. We calculated organ dose conversion coefficients for head, chest, abdomen and pelvis, and chest-abdomen-pelvis scans, and compared the results with the existing data calculated from Caucasian phantoms. We derived representative organ doses for Korean adults using Korean CT dose surveys combined with the dose conversion coefficients. The organ dose conversion coefficients from the Korean adult phantoms were slightly greater than those of the ICRP reference phantoms: up to 13% for the brain doses in head scans and up to 10% for the dose to the small intestine wall in abdominal scans. We derived Korean representative doses to major organs in head, chest, and AP scans using mean $CTDI_{vol}$ values extracted from the Korean nationwide surveys conducted in 2008 and 2017. The Korean-specific organ dose conversion coefficients should be useful to readily estimate organ absorbed doses for Korean adult male and female patients undergoing CT scans.

1. Introduction

Computed tomography (CT) scans contribute substantial clinical benefits to patients in modern medicine. However, several direct evidence of adverse late effects from repeated CT scans [1–3] have drawn attention to the importance of monitoring radiation dose delivered to CT patients, which requires accurate dose estimation. CT dose descriptors such as CT Dose Index (CTDI) and Dose-Length Product (DLP) are available for dose monitoring purposes but those quantities are the amount of radiation dose delivered to cylindrical acrylic phantoms not to the patient's anatomy. Estimation of the potential risk of adverse health effects requires organ-level radiation dose delivered to CT patients. Patient dose from CT scans can be measured by using physical phantoms combined with dosimeters or calculated using computational phantoms and Monte Carlo radiation transport techniques. By using the latter approach, which is more flexible and cost-effective, several dose calculation methods and tools have been introduced [4–7]. However, the computational human phantoms, one of the key components in those CT dose calculation tools, are based on Caucasian anatomical data so whether or not the tools can be directly applied to different ethnic groups is unclear.

In the past years, many Korean-specific computational human phantoms have been reported. Lee et al. developed the first Korean adult male voxel phantom, KORMAN, in 2004 [8], which was followed by the first Korean adult female voxel phantom, KORWOMAN [9]. Both phantoms are based on Magnetic Resonance (MR) images of healthy volunteers. The same research team introduced more detailed adult male voxel phantoms, KTMAN1 and KTMAN2, which are based on MR and CT image sets, respectively [10]. Korea Electronics and Telecommunications Research Institute (ETRI) introduced a 21-year-old adult [11] and 7-year-old child [12] voxel phantoms based on whole body MR image sets. More recently, High Definition Reference Korean (HDRK) adult male [13] and female [14] voxel phantoms were reported, which were

* Corresponding author.
E-mail address: choonsik.lee@nih.gov (C. Lee).

https://doi.org/10.1016/j.net.2021.08.008

Table 1
Characteristics of the adult male and female Korean voxel phantoms used in the current study.

Phantoms	Age (year)	Gender	Height (cm)	Weight (kg)	Image Type	Voxel resolution (cm)	Voxel volume (cm^3)	Voxel array size
KORMAN	30	Male	170	68	MR	0.2 × 0.2 x 1.0	0.0400	250 × 120 x 170
ETRI Man	21	Male	176	67	MR	0.3 × 0.3 x 0.3	0.0270	167 × 87 x 613
KTMAN1	25	Male	172	65	MR	0.2 × 0.2 x 0.5	0.0200	300 × 150 x 344
KTMAN2	35	Male	172	68	CT	0.2 × 0.2 x 0.5	0.0200	300 × 150 x 344
HDRK Man	33	Male	171	68	Photo	0.198 × 0.198 x 0.209	0.0082	247 × 141 x 850
KORWOMAN	25	Female	160	55	MR	0.15 × 0.15 x 0.8	0.0180	300 × 150 x 200
HDRK Woman	26	Female	161	54	Photo	0.204 × 0.204 x 0.207	0.0086	261 × 109 x 825

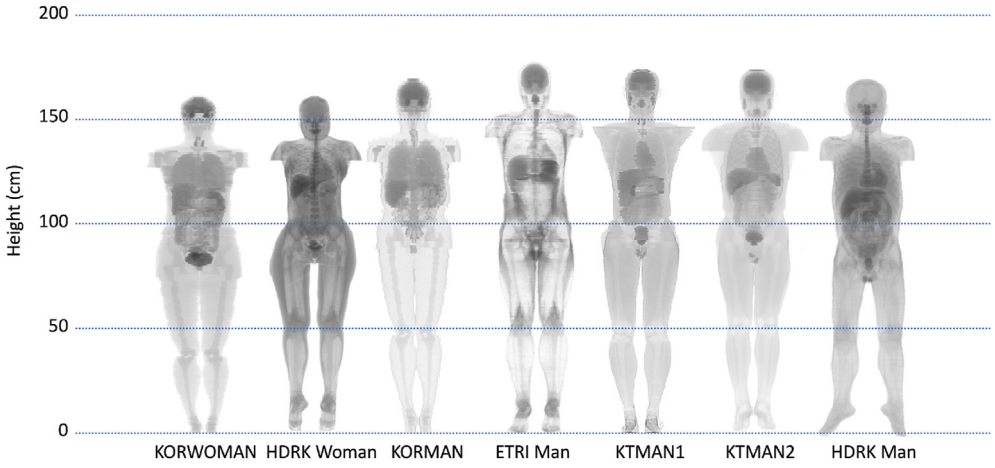

Fig. 1. Frontal projection views of the Korean adult male and female voxel phantoms adopted for CT dosimetry.

constructed from color slice images of adult cadavers. These realistic voxel phantoms representing the anatomy of Korean individuals can allow for Korean-specific organ dose estimation for CT scans.

In the current study, following the paper recently published on two sets of CT dose conversion coefficients by using pediatric (ETRI Child) and adult (ETRI Man) Korean voxel phantoms [15], we extended the study to include four Korean adult male and two Korean adult female voxel phantoms into CT organ dose calculations. We calculated major organ dose conversion coefficients for head, chest, abdomen and pelvis (AP), and chest-abdomen-pelvis (CAP) scans, and compared the results with the existing data calculated from Caucasian computational phantoms. We also derived Korean-representative organ dose levels for Korean adults based on Korean CT dose surveys combined with the organ dose conversion coefficients established in the current study.

2. Materials and methods

2.1. Computational human phantoms

We adopted four adult male voxel phantoms, KORMAN, KTMAN1, KTMAN2, and HDRK Man, and two adult female voxel phantoms, KORWOMAN and HDRK-Woman, to estimate organ dose in CT scans. Detailed information about the original source images used to construct voxel phantoms, body dimensions, voxel resolution, and 3D matrix size are summarized in Table 1. We also added the information of ETRI Man that we previously used [15] to Table 1 for comparison.

We modified the original voxel phantoms to accurately simulate

Table 2
Organ dose conversion coefficients (mGy/mGy) for **head CT scans** calculated from the Korean adult male and female phantoms. The average male and female data are shown in the last two columns.

Head Scan	Adult Male					Adult Female		Average	
	KORMAN	ETRI Man	KTMAN1	KTMAN2	HDRK Man	KORWOMAN	HDRK Woman	Male	Female
Brain	0.847	0.839	0.719	0.793	0.845	0.822	0.916	0.808	0.869
Thyroid	0.160	0.062	0.145	0.090	0.038	0.679	0.112	0.099	0.395
Lungs	0.009	0.004	0.007	0.008	0.004	0.013	0.010	0.007	0.012
SI wall	0.000	0.000	0.000	0.000	0.000	0.000	0.000	0.000	0.000
Colon wall	0.000	0.000	0.000	0.000	0.000	0.001	0.000	0.000	0.000
Stomach wall	0.001	0.000	0.001	0.001	0.000	0.002	0.001	0.001	0.002
Liver	0.001	0.000	0.001	0.002	0.001	0.002	0.002	0.001	0.002
Kidneys	0.001	0.000	0.000	0.001	0.000	0.001	0.000	0.000	0.000
Urinary Bladder	0.000	0.000	0.000	0.000	0.000	0.000	0.000	0.000	0.000
Heart	0.005	0.002	0.006	0.005	0.003	0.009	0.007	0.004	0.008
Esophagus	0.015	0.012	0.016	0.018	0.008	0.015	0.037	0.014	0.026
Spleen	0.002	0.000	0.001	0.002	0.000	0.002	0.001	0.001	0.001
Gonads	0.000	0.000	0.000	0.000	0.000	0.000	0.000	0.000	0.000

Table 3
Organ dose conversion coefficients (mGy/mGy) for **chest CT scans** calculated from the Korean adult male and female phantoms. The average male and female data are shown in the last two columns.

Organs	Adult Male					Adult Female		Average	
	KORMAN	ETRI Man	KTMAN1	KTMAN2	HDRK Man	KORWOMAN	HDRK Woman	Male	Female
Brain	0.017	0.067	0.009	0.014	0.015	0.015	0.019	0.024	0.017
Thyroid	1.081	1.056	0.284	1.725	2.027	0.309	1.275	1.235	0.792
Lungs	1.349	1.254	1.459	1.329	1.513	1.546	1.586	1.381	1.566
SI wall	0.173	0.079	0.118	0.088	0.042	0.066	0.052	0.100	0.059
Colon wall	0.213	0.039	0.076	0.157	0.036	0.087	0.058	0.104	0.073
Stomach wall	0.970	0.757	1.099	0.809	0.539	1.139	0.836	0.835	0.988
Liver	0.798	0.971	1.045	0.803	1.002	0.789	1.024	0.924	0.906
Kidneys	0.304	0.191	0.219	0.204	0.166	0.096	0.219	0.217	0.158
Urinary Bladder	0.009	0.006	0.006	0.003	0.002	0.001	0.001	0.005	0.001
Heart	1.383	1.217	1.629	1.460	1.525	1.561	1.581	1.443	1.571
Esophagus	1.201	0.909	1.164	1.225	1.396	1.392	1.204	1.179	1.298
Spleen	1.058	0.818	0.988	0.886	0.548	0.350	0.790	0.860	0.570
Gonads	0.002	0.001	0.002	0.001	0.000	0.002	0.002	0.001	0.002

Table 4
Organ dose conversion coefficients (mGy/mGy) for **abdomen-pelvis CT scans** calculated from the Korean adult male and female phantoms. The average male and female data are shown in the last two columns.

Organs	Adult Male					Adult Female		Average	
	KORMAN	ETRI Man	KTMAN1	KTMAN2	HDRK Man	KORWOMAN	HDRK Woman	Male	Female
Brain	0.001	0.045	0.001	0.001	0.000	0.001	0.001	0.010	0.001
Thyroid	0.012	0.004	0.011	0.019	0.016	0.018	0.025	0.013	0.021
Lungs	0.321	0.185	0.370	0.332	0.402	0.453	0.350	0.322	0.402
SI wall	1.333	1.426	1.634	1.636	1.540	1.667	1.730	1.514	1.699
Colon wall	1.204	1.364	1.608	1.410	1.416	1.620	1.543	1.400	1.581
Stomach wall	1.056	1.251	1.472	1.404	1.453	1.456	1.532	1.327	1.494
Liver	1.184	1.163	1.381	1.176	1.303	1.487	1.380	1.241	1.433
Kidneys	1.308	1.406	1.451	1.408	1.446	1.645	1.604	1.404	1.625
Urinary Bladder	0.703	0.815	1.403	1.121	0.461	1.546	0.458	0.901	1.002
Heart	0.353	0.369	0.261	0.415	0.219	0.580	0.509	0.323	0.544
Esophagus	0.246	0.419	0.310	0.231	0.226	0.364	0.422	0.286	0.393
Spleen	1.117	1.153	1.348	1.307	1.436	1.606	1.546	1.272	1.576
Gonads	0.061	0.215	0.112	0.071	0.048	1.255	1.157	0.101	1.206
Total skeleton	0.637	0.177	0.781	0.727	0.656	1.898	0.689	0.596	1.294

the posture of patients undergoing CT scans. To acquire better image quality, patients raise their arms for torso scans and lower the arms for head scans. To exclude the arms from both head and torso scans, we removed the arm structures from each phantom by manually erasing the skin, muscle, adipose, and skeleton included in the arms on axial phantom image slices by using a software, ImageJ (National Institutes of Health, Bethesda, MD). We kept the humeral heads and shoulders as the humeri include active bone marrow which is radiosensitive whereas active bone marrow does not exist in the removed part of the arms in adults [16]. Fig. 1 shows the frontal projection views of the voxel phantoms where the arms were removed. KTMAN1 did not have arms in its original format [10] so that we used the original phantom as is for CT dose calculations. The voxel phantom in binary format was converted into a lattice format to be imported to Monte Carlo calculation codes. The conversion was conducted using an in-house MATLAB script.

2.2. Organ dose conversion coefficients in CT scans

We employed the Monte Carlo radiation transport model of a reference CT scanner previously published [6]. The scanner simulation model was experimentally validated, which was published elsewhere [17–19]. The six voxel phantoms in binary file format were converted into ASCII format that is compatible with a general purpose Monte Carlo radiation transport code, MCNPX2.7 [20]. We recompiled MCNPX by implementing a user defined source routine to simulate the x rays emitted from the reference CT scanner. Organ absorbed dose per unit $CTDI_{vol}$, called organ dose conversion coefficients (mGy/mGy), were calculated for a series of consecutive slices from the top of the head to the bottom of the feet with the interval of 1 cm in each phantom. Considering the range of photon energy less than 120 kVp, we only scored kerma using *f6 tally without transporting secondary electrons assuming charged particle equilibrium. Default photon energy cutoff 1 keV was used and no variance reduction techniques were adopted. A total of ten million particles simulated for a single slice to achieve relative errors less than 1% for major organs. The supercomputing servers built in the National Institutes of Health were employed to conduct a large number of MCNP calculations. The total calculations of organ dose coefficients for all adult voxel phantoms took about two weeks. We used the x-ray energy spectrum of 120 kVp for all adult male and female phantoms. The x-ray spectra for the head and body bowtie filters were used for head and torso scans, respectively. The $CTDI_{vol}$ for 16-cm CTDI phantom was used for normalization of organ doses in head scans and that for 32-cm phantom used for torso scans including chest, AP, and CAP scans.

We derived organ dose conversion coefficients for head, chest, AP, and CAP scans from the slice-specific dose coefficients calculated from the Monte Carlo calculations. We adopted the scan coverage protocols used at the National Institutes of Health Clinical Center [6]. Head scans started from the top of the head to the second cervical vertebra. Chest scans ranged from the top of the clavicles to the middle level of the liver. AP scans covered the region from the top of the liver to the middle level of the femoral head.

Table 5
Organ dose conversion coefficients (mGy/mGy) for **chest-abdomen-pelvis CT scans** calculated from the Korean adult male and female phantoms. The average male and female data are shown in the last two columns.

Organs	Adult Male					Adult Female		Average	
	KORMAN	ETRI Man	KTMAN1	KTMAN2	HDRK Man	KORWOMAN	HDRK Woman	Male	Female
Brain	0.017	0.100	0.010	0.014	0.015	0.016	0.019	0.031	0.017
Thyroid	1.084	1.058	0.287	1.732	2.031	0.315	1.282	1.238	0.798
Lungs	1.406	1.290	1.501	1.405	1.594	1.635	1.661	1.439	1.648
SI wall	1.373	1.444	1.656	1.665	1.550	1.686	1.745	1.538	1.715
Colon wall	1.243	1.373	1.622	1.451	1.425	1.642	1.559	1.423	1.601
Stomach wall	1.261	1.405	1.636	1.591	1.563	1.661	1.685	1.491	1.673
Liver	1.359	1.405	1.566	1.369	1.538	1.645	1.631	1.447	1.638
Kidneys	1.378	1.448	1.487	1.473	1.490	1.673	1.665	1.455	1.669
Urinary Bladder	0.706	0.816	1.405	1.122	0.461	1.547	0.459	0.902	1.003
Heart	1.445	1.284	1.665	1.556	1.568	1.671	1.675	1.504	1.673
Esophagus	1.249	1.190	1.203	1.284	1.441	1.470	1.322	1.273	1.396
Spleen	1.351	1.274	1.493	1.507	1.547	1.687	1.694	1.435	1.690
Gonads	0.062	0.215	0.113	0.071	0.048	1.256	1.158	0.102	1.207

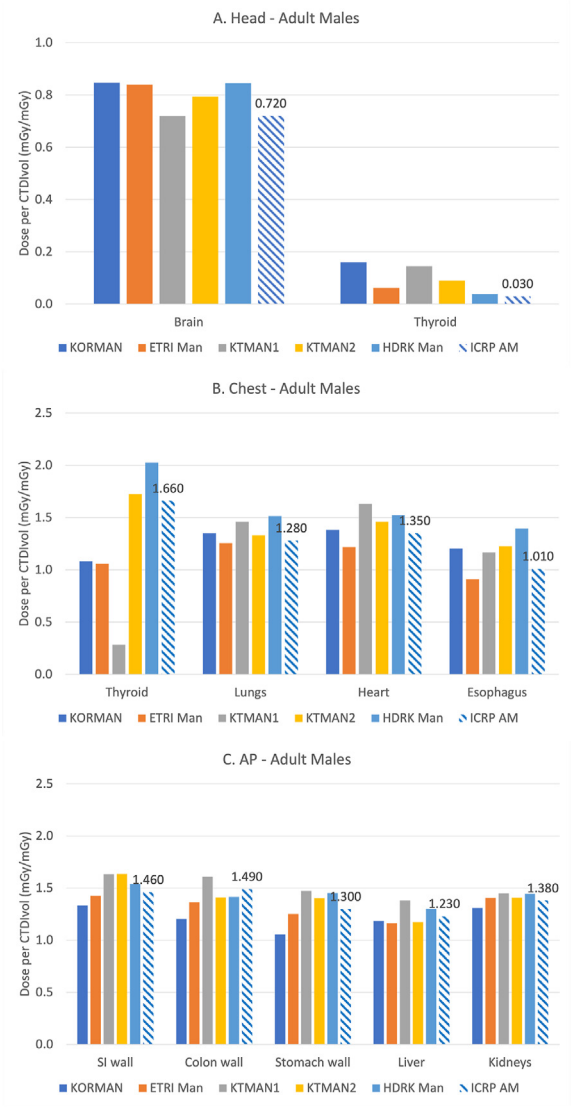

Fig. 2. Comparison of organ doses from (a) head, (b) chest, and (c) AP scans between Korean and ICRP **adult male** phantoms.

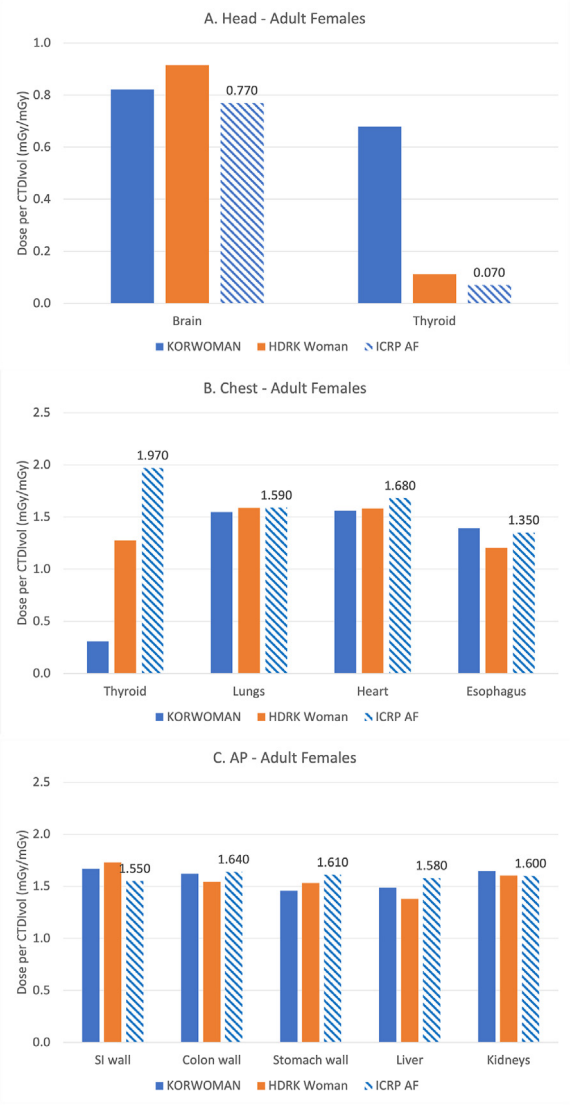

Fig. 3. Comparison of organ doses from (a) head, (b) chest, and (c) AP scans between Korean and ICRP **adult female** phantoms.

CAP scans combined the scan ranges of chest and AP scans. In each phantom, we manually selected the slices belonging to these scan coverage locations and added the dose conversion coefficients assigned to the slices to derive scan type-specific organ dose

Table 6
Effective diameter (cm) measured at the mid level of the scan range of head, chest, and abdomen-pelvis (AP) scans from the eight Korean voxel phantoms.

Phantoms	Effective Diameter (cm)		
	Head	Chest	AP
KORMAN	18	27	22
ETRI Man	17	26	24
KTMAN1	17	26	22
KTMAN2	16	28	23
HDRK Man	20	27	25
Korean Adult Male Average	18	27	23
KORWOMAN	15	22	19
HDRK Woman	17	22	22
Korean Adult Female Average	16	22	21
ICRP Adult Male	20	28	26
ICRP Adult Female	17	24	23

conversion coefficients. We also included the dose conversion coefficients from ETRI Man [15] to this study for comparison. Gender-averaged dose conversion coefficients were calculated for comparison. To analyze the degree of variation across the phantoms, we calculated coefficient of variation (COV), which is the ratio of the standard deviation to the mean.

To compare our results with those from Caucasian computational human phantoms, we used a software, National Cancer Institute dosimetry system for CT (NCICT) [6], which is based on the library of the International Commission on Radiological Protection (ICRP) reference pediatric [21] and adult [22] voxel phantoms. We calculated major organ doses for head, chest, and AP scans using NCICT and compared the results with the gender-averaged Korean dose conversion coefficients.

2.3. Measurement of effective diameter and organ depth

To better understand potential agreement or disagreement in organ doses in different computational phantoms, we measured two anatomical dimensions: effective diameter and organ depth.

Effective diameter is defined as the geometric mean of anteroposterior length and lateral length of a cross-sectional body contour [23]. Effective diameter is measured at the middle level of a given scan range. Effective diameter for a head scan, for example, is measured at the 10 cm from the top of the head if the head scan covers the length of 20 cm from the top of the head. We used ImageJ software to visualize cross-sectional views of each Korean phantom and measured effective diameters for different scan types: head, chest, and AP scans. We also measured effective diameters from the ICRP reference adult male and female voxel phantoms for comparison.

An organ's depth from the body's surface represents the amount of shielding that an organ has against CT x rays. To interpret the CT dose differences observed within these phantoms, we first measured the depth of fourteen organs within the Korean phantoms using methodology previously published in Griffin et al. [24] For the purposes of the current study, directions of organ depth calculation were sampled axially in the X–Y plane to represent the direction of incident, un-scattered photons from a CT fan beam in rotational geometry. Distance calculations from the voxels of the organ to the surface of the body were repeated 500,000 times, resulting in an organ depth distribution. Each distribution is characterized by depth bins of 1 mm width and the relative fraction of the organ at each depth, where the area underneath the plot sums to unity. Organ depths were also measured from the ICRP reference adult male and female voxel phantoms.

2.4. Calculation of Korean representative organ dose from CT

As an application of the Korean organ dose conversion coefficients established in the current study, we derived representative organ doses for Korean adults by combining our dose conversion coefficients with Korean survey data. We collected Korean $CTDI_{vol}$ from three national surveys performed in 2008 [25], 2012 [26], and 2017 [27]. In the most recent study in 2017, $CTDI_{vol}$ and DLP values were collected and analyzed for 13 CT examinations for adult patients and brain CT for pediatric patients (<2 year, 2–5 year, 6–10 year, and 11–15 year). The 2012 study was focused on pediatric patients. $CTDI_{vol}$ and DLP were analyzed for brain, chest, and abdomen CT by patient age group (newborn, <1 year, 2–5 year, 6–10 year, and >11 year). We used mean $CTDI_{vol}$ for adult patients from the 2008 and 2017 surveys and derived the dose to the brain in head scans, the lungs in chest scans, and the small intestine wall in AP scans by multiplying the $CTDI_{vol}$ with the organ dose conversion coefficients for Korean adult males and females.

3. Results

3.1. Korean organ dose conversion coefficients for CT scans

A comprehensive set of organ dose conversion coefficients (mGy/mGy), organ dose normalized to $CTDI_{vol}$, calculated from Korean adult male and female phantoms are tabulated in Tables 2–5 for head, chest, AP, and CAP scans, respectively. The brain shows the greatest dose coefficients in head scan (Table 2), which is followed by the thyroid. In chest scan (Table 3), the dose coefficients for the lungs are greatest and those for the heart follow the lungs. The kidneys show the largest dose coefficients both in AP and CAP scans as shown in Tables 4 and 5, respectively.

The female phantoms on average receive up to 16% (kidneys in AP scan) greater dose than the male phantoms for all scan types assuming identical $CTDI_{vol}$ used for males and females. The brain and lungs of the female phantoms show greater average dose coefficients than those of the male phantoms by 8% in head scans and 13% in chest scans. The thyroid shows the greatest variation both in head and chest scans with the COV of 77% (head scan) and 71% (chest scan) across the phantoms. The dose coefficients of the adult male heart show the second greatest variation in chest scan with the COV of 10.8%, where the dose coefficient ranges from 1.217 to 1.629 mGy/mGy (Table 3). The smallest variation of dose coefficients is observed in the adult female kidneys with the COV of 0.4%: 1.673 mGy/mGy from KORWOMAN and 1.665 mGy/mGy from HDRK Woman.

Some organs, located completely outside the scan range, still receive measurable doses. In chest scan, for example, the small intestine wall, which is outside the chest scan range (from the top of the clavicles to the middle level of the liver), shows the dose coefficients of 0.100 and 0.059 mGy/mGy for the Korean adult males and females, respectively (Table 3). The heart is not included in the AP scan range (from the middle level of the liver to the middle level of the femur) but shows dose coefficients of 0.323 and 0.544 mGy/mGy for the Korean males and females, respectively (Table 4).

3.2. Comparison with the ICRP reference phantom-based dose

Organ dose conversion coefficients from the Korean adult male and female phantoms were overall slightly greater than those of the ICRP reference phantoms (Figs. 2 and 3). Average brain doses in head scan from Korean adult male and female phantoms were greater than those from the ICRP adult male and female phantoms by 12% and 13%, respectively, as shown in Table 2 (Korean phantom

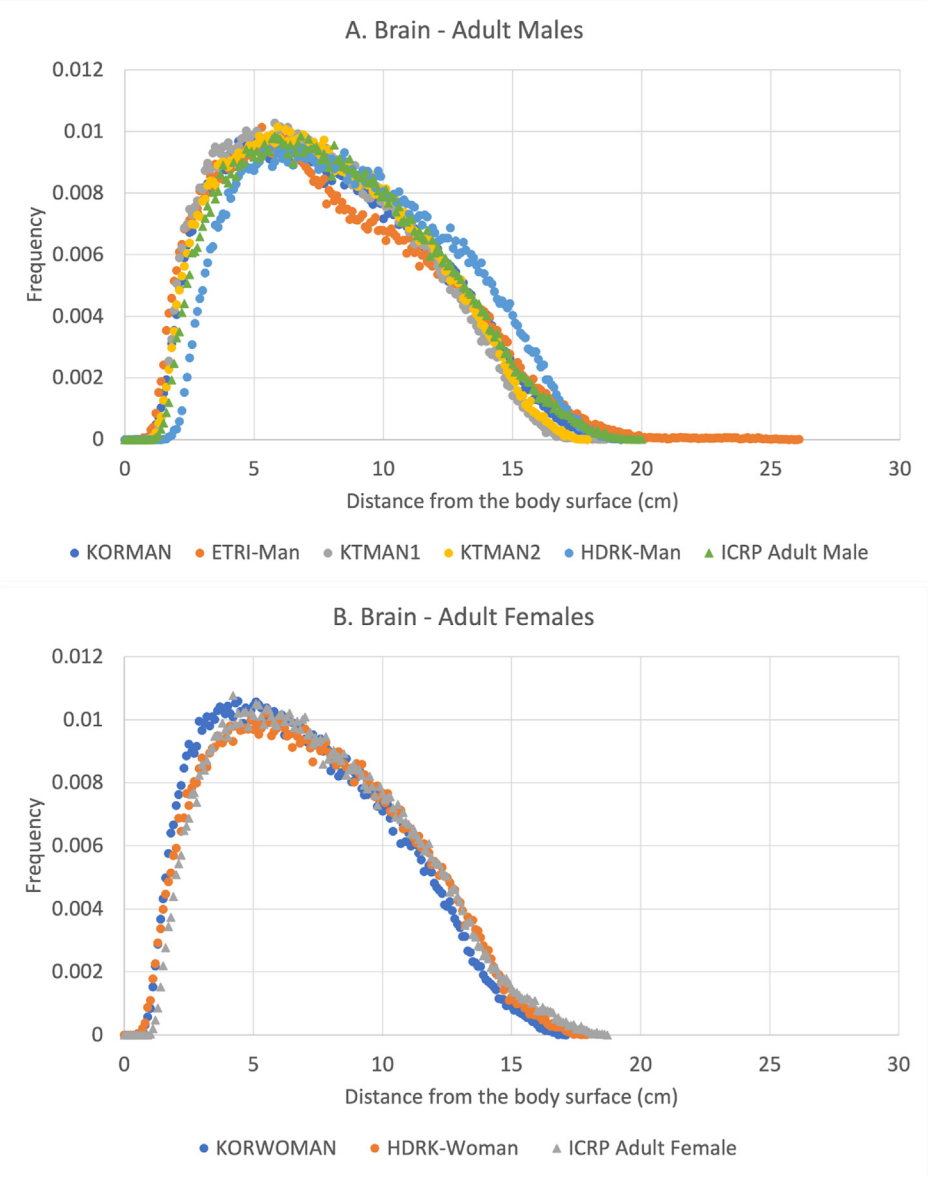

Fig. 4. Comparison of the depth of (a) brain, (b) lungs, and (c) colon from body surface in Korean pediatric and adult phantoms in rotational geometry.

average), and Fig. 2a (ICRP male phantom) and 3a (ICRP female phantom). The small intestine wall of the Korean male and female phantoms receive 4% and 10%, respectively, greater dose than that of the ICRP adult male and female phantoms in chest scan (Table 4, and Figs. 2c and 3c). In case of chest scans, however, the lungs of the Korean male phantoms on average receive 8% greater dose than those of the ICRP male phantom, whereas the average lung dose coefficient, 1.566 mGy/mGy, of the Korean female phantoms is slightly smaller than that of the ICRP adult female phantom, 1.590 mGy/mGy.

Effective diameter of the Korean phantoms is slightly smaller than that of the ICRP phantoms (Table 6). The average effective diameter from the Korean adult male phantoms was 18, 27, and 23 cm for head, chest, and AP scans, respectively, which are smaller than those of the ICRP adult male phantom by 1–3 cm. The Korean female phantoms also show slightly smaller than the ICRP adult female phantom by 1–2 cm on average.

Organ depth distribution of the brain (Fig. 4) and small intestine wall (Fig. 5), which show the greatest dose in head and AP scan, respectively, shows differences between the Korean and ICRP phantoms. The depth of the brain in the Korean male phantoms (Fig. 4a) is overall smaller than that of the ICRP adult male phantom except the brain of the HDRK-Man phantom of which depth is slightly greater than that of the ICRP male phantom. The similar trend is observed between the Korean female phantoms and the ICRP adult female phantom (Fig. 4b). The depth of the small intestine wall for the Korean phantoms are overall smaller than those of the ICRP phantoms for both males and females (Fig. 5).

3.3. Representative organ dose level for Korean adults

Dose to the major organs in head, chest, and AP scans were calculated using the mean $CTDI_{vol}$ extracted from the two Korean nationwide surveys in 2008 and 2017 (Table 3). Korean adult males and females might receive the lung dose of 8 and 9 mGy, respectively, from chest scan in 2017, which decreased from 14 to 16 mGy in 2008. The small intestine wall dose also decreased by about 40% from 2008 to 2017 both for the male and female. Brain dose of

Fig. 5. Comparison of the depth of (a) small intestine wall in the adult male phantoms and (b) small intestine wall in the adult female phantoms in rotational geometry.

males, however, increased from 41 mGy in 2008 to 46 mGy in 2017. The increase in brain dose is also observed in adult females: 44 mGy in 2008 to 50 mGy in 2017.

4. Discussion

The Korean adult female phantoms received overall smaller organ doses compared to the adult male phantoms. This can be explained by the difference in effective diameter between males and females (Table 6). The average effective diameter of the adult males are greater than that of the adult females by 2 cm in head and AP scans and by 5 cm in chest scan. The maximum difference in effective diameter between males and females is 6 cm in AP scan between HDRK Man (25 cm) and KORWOMAN (19 cm). Organ doses tend to decrease with increasing effective diameters due to the amount of shielding by overlaying muscle and adipose tissues against x rays from CT scanners [23].

The difference in organ dose between the Korean and ICRP phantoms can be also explained by the difference in effective diameter (Table 6). In addition to effective diameter, the difference in organ depth distribution (Figs. 4 and 5) between Korean and the ICRP phantoms helps analyze dose differences. The organs of ICRP phantoms seem to locate deeper from the body surface than those of the Korean phantoms. At the energy of 120 kVp, which was adopted in our CT simulations, the entrance region (depth from 0 to 5 cm) of the depth distribution in rotational geometry would have a bigger impact on dose than the exit region. The difference in organ depths between Korean and ICRP phantoms is clearly observed, especially, in the small intestine wall in adult females (Fig. 5b). The small intestine wall of KORWOMAN, for example, starts around 2 cm from the body surface whereas that of the ICRP adult female phantom starts around 4 cm after x rays enter the body surface.

As shown in COV, thyroid dose significantly varies in head (Table 2) and chest (Table 3) scans. In head scan, the thyroid of KORWOMAN (0.679 mGy/mGy) receives 18-fold greater dose than HDRK Man (0.038 mGy/mGy). It is reported that the vertical

location of the thyroid substantially varies in different individuals by up to 4 cm [28]. Depending on its location, the amount of volume included in head and chest scan coverage would substantially differ. In the same phantom, if a smaller portion of the thyroid is included in head scan coverage, a larger portion must be included in chest scan coverage and vice versa. This is shown in the case of HDRK Man, of which thyroid dose is smallest among other male phantoms in head scan (Table 2) but greatest in chest scan (Table 3).

We are aware of the following limitations of the current study. First, we only adopted five adult male and two adult female computational phantoms in the calculation of dose conversion coefficients. It is obvious that more sample size would provide more generalizable results. However, these seven adult phantoms are the only computational phantoms based on Korean tomographic images to date. Considering tremendous time and labor taken to develop voxel phantoms, the current study includes the largest number of computational human phantoms for CT dose calculations within an ethnic group. Second, we did not account for tube current modulation in organ dose calculations. We expect our organ dose conversion coefficients may slightly overestimate the dose to the organs in chest and abdomen regions and underestimate the dose to the organs near the shoulder and pelvic regions [6].

5. Conclusion

We established a library of organ dose conversion coefficients for Korean adult males and females undergoing CT scans by using seven Korean adult computational phantoms combined with Monte Carlo radiation transport techniques. The organ dose conversion coefficients from the Korean adult male and female phantoms were overall slightly greater than those of the ICRP reference phantoms. The Korean-specific organ dose conversion coefficients should be useful to readily estimate organ absorbed doses for Korean adult male and female patients undergoing CT scans.

Declaration of competing interest

The authors declare that they have no known competing financial interests or personal relationships that could have appeared to influence the work reported in this paper.

Acknowledgement

This research was funded by the intramural research program of the National Institutes of Health, National Cancer Institute, Division of Cancer Epidemiology and Genetics.

References

[1] M.S. Pearce, J.A. Salotti, M.P. Little, K. McHugh, C. Lee, K.P. Kim, N.L. Howe, C.M. Ronckers, P. Rajaraman, A.W. Sir Craft, L. Parker, A. Berrington de González, Radiation exposure from CT scans in childhood and subsequent risk of leukaemia and brain tumours: a retrospective cohort study, Lancet 380 (2012) 499–505, https://doi.org/10.1016/S0140-6736(12)60815-0.

[2] J.D. Mathews, A.V. Forsythe, Z. Brady, M.W. Butler, S.K. Goergen, G.B. Byrnes, G.G. Giles, A.B. Wallace, P.R. Anderson, T.A. Guiver, P. McGale, T.M. Cain, J.G. Dowty, A.C. Bickerstaffe, S.C. Darby, Cancer risk in 680,000 people exposed to computed tomography scans in childhood or adolescence: data linkage study of 11 million Australians, Br. Med. J. 346 (2013) 2360–f2360, https://doi.org/10.1136/bmj.f2360.

[3] J.M. Meulepas, C.M. Ronckers, A.M.J.B. Smets, R.A.J. Nievelstein, P. Gradowska, C. Lee, A. Jahnen, M. van Straten, M.-C.Y. de Wit, B. Zonnenberg, W.M. Klein, J.H. Merks, O. Visser, F.E. van Leeuwen, M. Hauptmann, Radiation exposure from pediatric CT scans and subsequent cancer risk in The Netherlands, J. Natl. Cancer Inst. 111 (2019) 256–263, https://doi.org/10.1093/jnci/djy104.

[4] G. Stamm, H.D. Nagel, CT-expo–a novel program for dose evaluation in CT, ROFO. Fortschr. Geb. Rontgenstr. Nuklearmed. 174 (2002) 1570–1576, https://doi.org/10.1055/s-2002-35937.

[5] ImPACT, ImPACT CT Patient Dosimetry Calculator, 2011. London, UK, http://www.impactscan.org/ctdosimetry.htm.

[6] C. Lee, K.P. Kim, W.E. Bolch, B.E. Moroz, Les Folio, NCICT: a computational solution to estimate organ doses for pediatric and adult patients undergoing CT scans, J. Radiol. Prot. 35 (2015) 891–909, https://doi.org/10.1088/0952-4746/35/4/891.

[7] X. Li, E. Samei, W.P. Segars, G.M. Sturgeon, J.G. Colsher, D.P. Frush, Patient-specific dose estimation for pediatric chest CT, Med. Phys. 35 (2008) 5821–5828, https://doi.org/10.1118/1.3026593.

[8] C. Lee, J. Lee, Korean adult male voxel model KORMAN segmented from magnetic resonance images, Med. Phys. 31 (2004) 1017–1022.

[9] C. Lee, Construction of Korean Adult Voxel Phantoms for Radiation Dosimetry and Their Applications, Hanyang University, 2002.

[10] C. Lee, S. Park, J.K. Lee, Development of the two Korean adult tomographic models, Med. Phys. 33 (2006) 380–390.

[11] A. Lee, W.Y. Choi, M.S. Chung, H. Choi, J. Choi, Development of Korean male body model for computational dosimetry, ETRI J 28 (2006) 107–110.

[12] A.K. Lee, J.K. Byun, J.S. Park, H.D. Choi, J. Yun, Development of 7-year-old Korean child model for computational dosimetry, ETRI J 31 (2009) 237–239.

[13] C.H. Kim, S.H. Choi, J.H. Jeong, C. Lee, M.S. Chung, HDRK-Man: a whole-body voxel model based on high-resolution color slice images of a Korean adult male cadaver, Phys. Med. Biol. 53 (2008) 4093–4106, https://doi.org/10.1088/0031-9155/53/15/006.

[14] Y.S. Yeom, J.H. Jeong, C.H. Kim, M.C. Han, B.K. Ham, K.W. Cho, S.B. Hwang, HDRK-Woman: whole-body voxel model based on high-resolution color slice images of Korean adult female cadaver, Phys. Med. Biol. 59 (2014) 3969–3984, https://doi.org/10.1088/0031-9155/59/14/3969.

[15] T. Won, A.-K. Lee, H. Choi, C. Lee, Radiation dose from computed tomography scans for Korean pediatric and adult patients, J. Radiat. Prot. Res. (2021), https://doi.org/10.14407/jrpr.2021.00010.

[16] ICRP, Basic anatomical and physiological data for use in radiological protection : reference values, ICRP Publ. 89 Ann ICRP. 32 (2002) 1–277.

[17] D.J. Long, C. Lee, C. Tien, R. Fisher, M.R. Hoerner, D. Hintenlang, W.E. Bolch, Monte Carlo simulations of adult and pediatric computed tomography exams: validation studies of organ doses with physical phantoms, Med. Phys. 40 (2013) 13901, https://doi.org/10.1118/1.4771934.

[18] J. Dabin, A. Mencarelli, D. McMillan, A. Romanyukha, L. Struelens, C. Lee, Validation of calculation algorithms for organ doses in CT by measurements on a 5 year old paediatric phantom, Phys. Med. Biol. 61 (2016) 4168–4182, https://doi.org/10.1088/0031-9155/61/11/4168.

[19] L. Giansante, J.C. Martins, D.Y. Nersissian, K.C. Kiers, F.U. Kay, M.V.Y. Sawamura, C. Lee, E.M.M.S. Gebrim, P.R. Costa, Organ doses evaluation for chest computed tomography procedures with TL dosimeters: comparison with Monte Carlo simulations, J. Appl. Clin. Med. Phys. 20 (2019) 308–320, https://doi.org/10.1002/acm2.12505.

[20] D.B. Pelowitz, MCNPX User's Manual Version 2.7.0, Los Alamos National Laboratory, 2011.

[21] ICRP, Paediatric Reference Computational Phantoms, ICRP Publ. 143 Ann ICRP, 2020.

[22] ICRP, Adult Reference Computational Phantoms, ICRP Publ, 2009, pp. 1–166, 110 Ann ICRP. 39.

[23] J.M. Boone, K.J. Strauss, D.D. Cody, C.H. McCollough, M.F. McNitt-Gray, T.L. Toth, Size-specific Dose Estimates (SSDE) in Pediatric and Adult Body CT Examinations, AAPM, 2011. https://www.aapm.org/pubs/reports/RPT_204.pdf.

[24] K.T. Griffin, T.A. Cuthbert, S.A. Dewji, C. Lee, Stylized versus voxel phantoms: a juxtaposition of organ depth distributions, Phys. Med. Biol. 65 (2020), 065007, https://doi.org/10.1088/1361-6560/ab7686.

[25] Ministry of Food and Drug Safety, National Survey of Radiation Dose of Computed Tomography in Korea, 2008.

[26] Ministry of Food and Drug Safety, Establishment of Diagnostic Reference Level in Pediatric Computed Tomography in Korea, 2012.

[27] Korea Centers for Disease Control and Prevention, Diagnostic Reference Levels of Computed Tomography, national survey, 2017.

[28] Y.S. Yeom, D. Villoing, N. Greenstein, C.M. Kitahara, L.R. Folio, C.H. Kim, C. Lee, Investigation OF the influence OF thyroid location ON iodine-131 S values, Radiat. Prot. Dosimetry. 189 (2020) 163–171, https://doi.org/10.1093/rpd/ncaa027.